1521-0103/354/1/65–72$25.00
THE JOURNAL OF PHARMACOLOGY AND EXPERIMENTAL THERAPEUTICS

http://dx.doi.org/10.1124/jpet.115.223891
J Pharmacol Exp Ther 354:65–72, July 2015

The Journal of PHARMACOLOGY And Experimental Therapeutics

Dosing Time-Dependent Changes in the Analgesic Effect of Pregabalin on Diabetic Neuropathy in Mice

Takahiro Akamine, Satoru Koyanagi, Naoki Kusunose, Hana Hashimoto, Marie Taniguchi, Naoya Matsunaga, and Shigehiro Ohdo

Department of Pharmaceutics, Faculty of Pharmaceutical Sciences, Kyushu University, Fukuoka, Japan

Received March 15, 2015; accepted May 11, 2015

ABSTRACT

Patients with diabetes often develop peripheral nerve complications, including numbness and pain in the extremities. Diabetes-induced peripheral neuropathic pain is characterized by hypersensitivity to innocuous stimuli, known as tactile allodynia. Pregabalin (PGN) is currently used to treat diabetes-induced peripheral neuropathy and alleviates allodynia. In the present study, we demonstrated that the antiallodynic effect of PGN on diabetic mice was modulated by circadian changes in its intestinal absorption. A single intraperitoneal administration of 200 mg/kg streptozotocin (STZ) to mice induced type I diabetic pathologic changes that were accompanied by tactile allodynia. The intensity of tactile allodynia in STZ-induced diabetic mice was alleviated by the oral administration of PGN; however, the antiallodynic effect varied according to its dosing time. The analgesic effect of PGN was enhanced by its administration at the times of day when its intestinal absorption was accelerated. Organic cation transporter novel type 1 (Octn1) mediated the uptake of PGN into intestinal epithelial cells. The expression of Octn1 in the small intestine of STZ-induced diabetic mice oscillated in a circadian time-dependent manner. This oscillation in Octn1 appeared to cause the time of day-dependent changes in the intestinal absorption of PGN. Similar dosing time dependencies of the antiallodynic effect of PGN and oscillation in Octn1 expression were also detected in type II diabetic db/db mice. These results suggested that the dosing time-dependent differences in the analgesic effect of PGN were attributable to circadian oscillations in the intestinal expression of Octn1 and also that optimizing its dosing schedule may assist in achieving rational pharmacotherapy for diabetes-induced peripheral neuropathic pain.

Introduction

Peripheral neuropathy is a major complication of diabetes. The main symptoms of diabetic peripheral neuropathy are numbness and/or pain in the extremities. Many patients with diabetic peripheral neuropathy have severe pain. The mainstay treatment of diabetes-induced neuropathic pain is pharmacotherapy. Pregabalin [PGN; (*S*)-3-(aminomethyl)-5-methylhexanoic acid] is now widely used to alleviate diabetic peripheral neuropathy and fibromyalgia (Parker et al., 2015). The analgesic effects of PGN have been associated with the modulation of neurotransmitter release or neuronal excitability due to alterations in Ca^{2+} currents (Dooley et al., 2002; Kavoussi, 2006). PGN has been shown to modulate Ca^{2+} currents by binding to the $\alpha 2\delta$-1 subunit of voltage-dependent Ca^{2+} channels (Fink et al., 2002). However, patients with diabetic neuropathy and fibromyalgia are sometimes refractory to PGN treatments (Rosenstock et al., 2004).

One approach to increase the effects of pharmacotherapy is the administration of drugs at times of day when they are most effective and/or best tolerated (Lévi et al., 1997; To et al., 2011). Circadian variations in biologic functions such as gene expression and protein synthesis are important factors that affect the efficacy of drugs. The expression and function of some types of proteins that regulate susceptibility to drugs and their pharmacokinetics were previously reported to change in a circadian time-dependent manner (Ohdo et al., 2001; Gachon et al., 2004; Lemmer, 2005). Therefore, the pharmacologic effects of PGN may be further improved by optimizing the dosing schedule. In the present study, we investigated the influence of the dosing time of PGN on its analgesic effects in an animal model of diabetes-induced neuropathic pain. The analgesic effects of PGN were changed by its oral administration time, which were associated with circadian change in the intestinal absorption process. Circadian oscillation in the intestinal expression of several types of xenobiotic transporter has been identified in laboratory animals (Murakami et al., 2008; Hamdan et al., 2012; Okamura et al., 2014). Recently, we also found that intestinal

This work was partially supported by a Grant-in-Aid for Scientific Research (A) [25253038 (to S.O.)]; a Grant-in-Aid for Scientific Research (B) [24390149 15H04765 (to S.K.)]; and a Grant-in-Aid for Challenging Exploratory Research [25670079 (to S.O.); 26670317 (to S.K.)] from the Japan Society for the Promotion of Science.
dx.doi.org/10.1124/jpet.115.223891.

ABBREVIATIONS: AUC, area under the curve of the serum concentration-time curve; ERGO, ergothioneine; HPLC, high-performance liquid chromatography; NONMEM, nonlinear mixed effect model; OBJ, objective function; Octn1, organic cation transporter novel-1; PBS, phosphate-buffered saline; PCR, polymerase chain reaction; PGN, pregabalin; PWT, paw withdrawal test; siRNA, small interfering RNA; STZ, streptozotocin; ZT, zeitgeber time.

expression of organic cation transporter novel type 1 (Octn1) in mice oscillated in a circadian time-dependent manner (Wada et al., 2015). Although the mechanism of intestinal absorption of PGN has not been identified, we also demonstrated that Octn1 mediated the uptake of PGN into intestinal epithelial cells. Therefore, the mechanism underlying dosing time-dependent changes in the analgesic effects of PGN was explored by focusing on circadian property of intestinal expression of Octn1 in type I and type II diabetic model mice.

Materials and Methods

Animals and Treatment. Five-week-old male ICR mice were purchased from Charles River Japan Inc. (Kanagawa, Japan). Five-week-old male BKS.Cg-m^{+}*Lepr^{db}*/+*Lepr^{db}*/Jcl (db/db) mice and age/sex-matched BKS.Cg-m^{+}/m^{+}/Jcl (wild-type) mice were purchased from CLEA Japan Inc. (Tokyo, Japan). Mice were housed in a light-controlled room at a room temperature of 24 ± 1°C and humidity of 60 ± 10% with food and water available ad libitum. Under the light/dark cycle, zeitgeber time (ZT) 0 was designated as lights on and ZT12 as lights off. Animals were treated in accordance with the guidelines stipulated by the Animal Care and Use Committee of Kyusyu University. Pregabalin (PGN; Pfizer, Tokyo, Japan) was dissolved in saline and injected in a volume of 0.1 ml/10 g body weight.

Preparation of the Type I Diabetic Neuropathic Pain Model. We used the experimental model of type I diabetes, the streptozotocin (STZ; Wako, Osaka, Japan)-induced diabetic mouse. The STZ-induced diabetes was induced in ICR mice by the single administration of STZ (200 mg/kg i.p.), a pancreatic β-cell toxin. Body weight and blood glucose levels were assessed after the STZ treatment. Blood glucose levels were determined by an optical reflectance spectroscopy method. Control mice were injected with an equal volume of saline.

Assessment of Diabetes-Induced Neuropathic Pain. Diabetes-induced neuropathic pain was assessed using von Frey filaments (0.02–2.0 g; Muromachi Kikai Co., Ltd., Tokyo, Japan). Mice were placed in plastic cages with a wire mesh floor and allowed to acclimate for 30 minutes before hindpaw mechanical thresholds were tested. The paw withdrawal threshold (PWT) was assessed by the up-down method (Chaplan et al., 1994). To evaluate the alleviation effects of PGN on diabetes-induced neuropathic pain, the area under the curve (AUC) of the PWT was calculated using the trapezoidal rule over the entire time course of the PWT.

Measurement of PGN Concentrations. The concentrations of PGN in serum and cell lysates were determined by high-performance liquid chromatography (HPLC). Gabapentin (Tokyo Chemical Industry Co. Ltd., Tokyo, Japan) was used as the internal standard. They were derivatized with *O*-phthaldialdehyde (Wako) as described previously (Vermeij and Edelbroek, 2004). The mobile phase of phosphate buffer (pH 3.0; 20 mM)-acetonitrile (3:1, v/v) was flowed at 1.0 ml/min through a 5C_{18}-MS-II column (4.6 × 150 mm; Nacalai Tesque Co., Ltd., Kyoto, Japan) using a pump (LC-20AD; Shimadzu, Kyoto, Japan). The separated analyte was detected using the Spectrofluorometric Detector RF-20Axs (excitation and emission at 330 and 450 nm, respectively; Shimadzu). The total run time was 30 minutes, with PGN and gabapentin eluting at 20 and 28 minutes, respectively. Serum concentration of PGN was expressed as micromoles per liter. The intestinal and cellular accumulation of PGN was expressed as nanomoles per milligram of protein.

Pharmacokinetic Analysis. Serum concentrations of PGN were analyzed using the nonlinear mixed effect model (NONMEM) program (ICON, Dublin, Ireland). NONMEM is a computer program designed to analyze pharmacokinetics in study populations by pooling data. Population pharmacokinetic parameters were calculated using 58 serum PGN concentrations obtained from 58 mice after the one-compartment model with first-order absorption (the PREDPP program, subroutines ADVAN2 and TRANS2). Bayesian estimates of individual pharmacokinetic parameters were obtained by the post hoc method of the NONMEM program. The improvement in fit obtained with the addition of a covariate was assessed by changes in the objective function (OBJ). At the assessing step, OBJ values were compared between each model. A difference in the −2 log likelihood difference was asymptotically distributed as χ^2 with degrees of freedom equal to the number of parameters. A difference of 3.841 in the value of OBJ with freedom 1 was accepted as significant ($P < 0.05$).

Transport Study of PGN Using aMoS7 Cells. Immortalized small intestine epithelial cells (aMoS7), established from adult mouse intestinal crypts (Iwamoto et al., 2011), were kindly provided by Dr. Totsuka (Tokyo University). We recently demonstrated the functional expression of Octn1 in aMoS7 cells (Wada et al., 2015) and used the cells to investigate whether intestinal absorption of PGN was mediated via Octn1. Cells were maintained in Dulbecco's modified Eagle's medium (Sigma-Aldrich, St. Louis, MO) supplemented with 10% fetal bovine serum (Sigma-Aldrich), 25 U/ml of penicillin (Gibco, Gaithersburg, MD), 25 μg/ml of streptomycin (Gibco), and 10 μg/ml of insulin (Wako).

For downregulation of Octn1 in aMoS7 cells, we designed small interfering RNA (siRNA) for knockdown experiments using BLOCK-iTTM RNAi Designer (https://rnaidesigner.invitrogen.com/rnaiexpress/). The target sequence of the mouse *Slc22a4* was as follows: GUUGGUACCGACACGUCUGACCUAA (GenBank accession no. NM_019687). The oligonucleotides were transfected into aMoS7 cells at a final concentration of 10, 50, or 100 pmol/well using Lipofectamine 2000 reagent (Invitrogen/Life Technologies, Carlsbad, CA). To establish Octn1 overexpressing cells, the full-length of mouse *Slc22a4* cDNA was subcloned into the BamHI and XhoI sites of pcDNA3.1 vectors (Invitrogen/Life Technologies), and the constructs were transfected into aMoS7 cells. Transgene expressing cells were selected with G418 (Wako), and individual colonies were expanded and maintained in media containing 4 μg/ml G418. The total amount of siRNA per well was adjusted by adding control siRNA. Up- or downregulation of Octn1 was confirmed by Western blotting.

To perform the transport experiment, aMos7 cells were preincubated for 30 minutes at 37°C with 2 ml of transport medium containing 115 mM NaCl, 2.5 mM KCl, 1 mM $CaCl_2$, 1 mM $MgSO_4$ $7H_2O$, 10 mM HEPES, 5 mM glucose (pH 7.4). After preincubation, cells were incubated with 2 ml of PGN solution (30 mM; PGN dissolved in transport medium) at indicated times. After being incubated, the cells were rinsed twice with ice-cold phosphate-buffered saline (PBS). Thereafter, cells were homogenized in PBS, and the concentrations of PGN in the homogenate were measured by HPLC. The transport experiment was also performed in the presence or absence of ergothioneine (ERGO), a typical substrate of Octn1 (Gründemann et al., 2005). In sodium-free experiments, sodium ions in transport medium were replaced with *N*-methylglucamine, and cells obtained were suspended in sodium-free medium.

Determination of Intestinal Accumulation of PGN. Proximal segments of the jejunum were isolated from STZ-induced diabetic mice at ZT2 and ZT14. The isolated intestinal segments were flushed with ice-cold saline and preincubated at 37°C for 20 minutes in Krebs-Ringer buffer (128.9 mM NaCl, 4.2 mM KCl, 1.5 mM $CaCl_2$, 22.4 mM $NaHCO_3$, 1.2 mM KH_2PO_4, 1.3 mM $MgSO_4$, 10 mM D-glucose) that was equilibrated with 95% O_2, 5% CO_2. After the preincubation, PGN was added to the buffer at a final concentration of 0.5 mM, and the segments were incubated at 37°C for 30 minutes in the presence or absence of 0.5 mM ERGO. After the incubation, segments were rinsed with ice-cold PBS and homogenized in 300 ml PBS. The concentrations of PGN in the homogenate were measured by HPLC.

RNA Extraction and Quantitative Real-Time Polymerase Chain Reaction Analysis. RNA was extracted using RNAiso reagent (Takara Bio Co., Ltd., Otsu, Japan). cDNA was synthesized using a ReverTra Ace qPCR RT kit (Toyobo, Osaka, Japan) and amplified by polymerase chain reaction (PCR). A real-time PCR analysis was performed on diluted cDNA samples using THUNDERBIRD SYBR

qPCR Mix (Toyobo) with the 7500 real-time PCR system (Applied Biosystems, Foster City, CA). Data were normalized to β-actin mRNA as a control. The sequences of the mouse *Slc22a4* primers were as follows: 5′-AGAAAGCCGCAAAGATGAACAG-3′ and 5′-GGTTAGCATCCACAGCATCAC-3′. The sequences of the mouse *Actin* primers (internal control) were as follows: 5′-CACACCTTCTACAATGAGCTGC-3′ and 5′-CATGATCTGGGTCATCTTTTCA-3′.

Western Blotting. The spinal cord or small intestine was removed from mice and homogenized in CelLytic MT Cell Lysis Reagent (Sigma-Aldrich)-supplemented protease inhibitor cocktail, which contained 2 μg/ml leupeptin, 100 μM phenylmethanesulfonyl fluoride, and 200 μM sodium vanadate. After centrifugation at 12,000*g* for 10 minutes, the supernatant proteins were separated on sodium dodecyl sulfate-polyacrylamide gels and transferred to a polyvinylidene difluoride membrane. The membranes were reacted with antibodies against the mouse $\alpha 2\delta$-1 subunit (Alomone Laboratories, Jerusalem, Israel), Octn1 (Alpha Diagnostic International, San Antonio, TX), or Actin (Santa Cruz Biotechnology, Santa Cruz, CA). Specific antigen-antibody complexes were visualized using horseradish peroxidase–conjugated secondary antibodies and Chemi-Lumi One (Nacalai Tesque).

Statistical Analysis. The 0.05 level of probability was taken as the criterion for significance. The significance of differences was analyzed by analysis of variance and Fisher's least significant difference test among multiple groups.

Results

Influence of the Dosing Time on Analgesic Effects of PGN in STZ-Induced Diabetic Mice. To develop a diabetic neuropathy animal model, ICR mice were administered a single dosage of STZ (200 mg/kg i.p.). This bacterium-derived toxin is known to ablate pancreatic β-cells and induce insulin deficiency. Therefore, STZ-induced hyperglycemic animals are often used as a type I diabetic model (Blay et al., 1985). Blood glucose levels were markedly increased on day 3 after the STZ treatment (Fig. 1A), and gain of body weight was suppressed in STZ-treated mice (Fig. 1B). The PWT of STZ-induced diabetic mice decreased gradually and reached trough levels at day 14 after the STZ treatment (Fig. 1C).

To investigate whether the analgesic effects of PGN varied according to its dosing time, STZ-induced diabetic mice were orally administered 50 mg/kg of PGN at ZT2 or ZT14 on day 21 after the STZ treatment. The dosing time points were selected based on our previous findings in a nerve-injured neuropathic pain model (Kusunose et al., 2010). Although the PWT of STZ-induced diabetic mice was transiently increased after the PGN administration at both dosing time points, the analgesic effects of PGN were more effective in mice treated at ZT14 than at ZT2 (Fig. 2A). On the other hand, no significant dosing time-dependent difference was observed in the analgesic effects of PGN after its intraperitoneal administration (50 mg/kg) at ZT2 and ZT14 (Fig. 2B).

A pharmacokinetic study was performed in STZ-induced diabetic mice on day 21 after the STZ treatment to determine the underlying mechanism of the dosing time-dependent difference in the analgesic effects of PGN. Serum concentrations of PGN peaked 0.5 hour after its oral administration at both ZT2 and ZT14 (50 mg/kg); however, the peak concentration of PGN was significantly higher in mice administered PGN at ZT14 than at ZT2 (Fig. 2C). On the other hand, no significant dosing time-dependent difference was observed in the time course of serum concentrations of PGN after its intraperitoneal administration (50 mg/kg) at ZT2 and ZT14 (Fig. 2D). These results suggest that the dosing time-dependent difference in the analgesic effects of PGN is related to its pharmacokinetics.

By using population parameters, the individual pharmacokinetic parameters of PGN were calculated based on Bayesian estimates, and the AUC and half-life were then derived from the values obtained (Table 1). The value of the absorption rate constant (k_a) was significantly larger in STZ-induced diabetic mice orally administered PGN at ZT14 than at ZT2 ($P < 0.01$), whereas no significant dosing time-dependent difference was observed in the other pharmacokinetic parameters.

Octn1 Mediates the Time-Dependent Uptake of PGN into the Small Intestine of STZ-Induced Diabetic Mice. PGN is a structural analog of gabapentin (Vermeij and Edelbroek, 2004). We recently reported that gabapentin was taken into intestinal epithelial cells by Octn1 (Wada et al., 2015). However, there is currently no direct evidence for the contribution of Octn1 to the transport of PGN. Therefore, we determined whether Octn1 mediated the incorporation of PGN into intestinal epithelial cells. Substantial expression of Octn1 was detected in immortalized mouse intestine epithelial cells aMoS7 (Fig. 3A, left). Transfection of cells with Octn1-expressing vectors resulted in elevation of its protein level. Because transfection with empty vectors (pcDNA3.1) had little effect on the expression of Octn1 protein in aMoS7 cells, we compared the ability of native and Octn1-overexpressing aMoS7 cells to uptake PGN. Incubation of native aMoS7 cells with PGN (30 mM) used significant

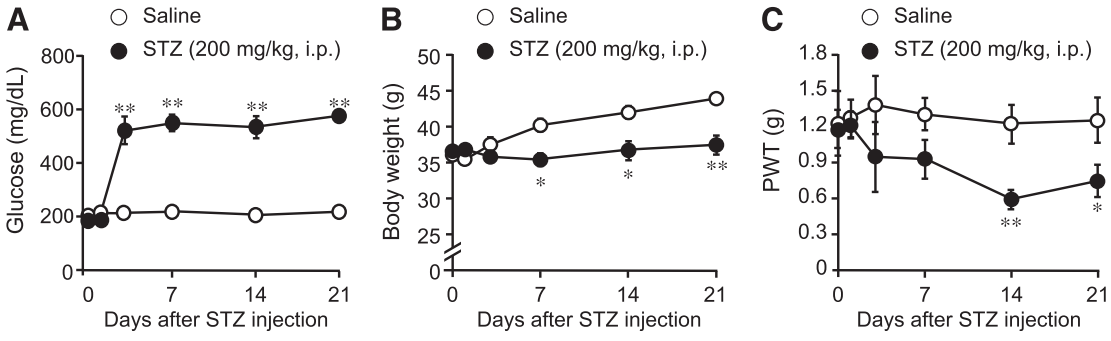

Fig. 1. Development of diabetic neuropathy in STZ-treated mice. The time courses of blood glucose levels (A), gain of body weight (B), and PWT (C) in STZ-treated mice. Mice were administrated STZ intraperitoneally (200 mg/kg). Values are shown as means with S.E.M. (n = 6 or 7). $^{**}P < 0.01$, $^{*}P < 0.05$, significantly different from saline-treated mice at the corresponding time points.

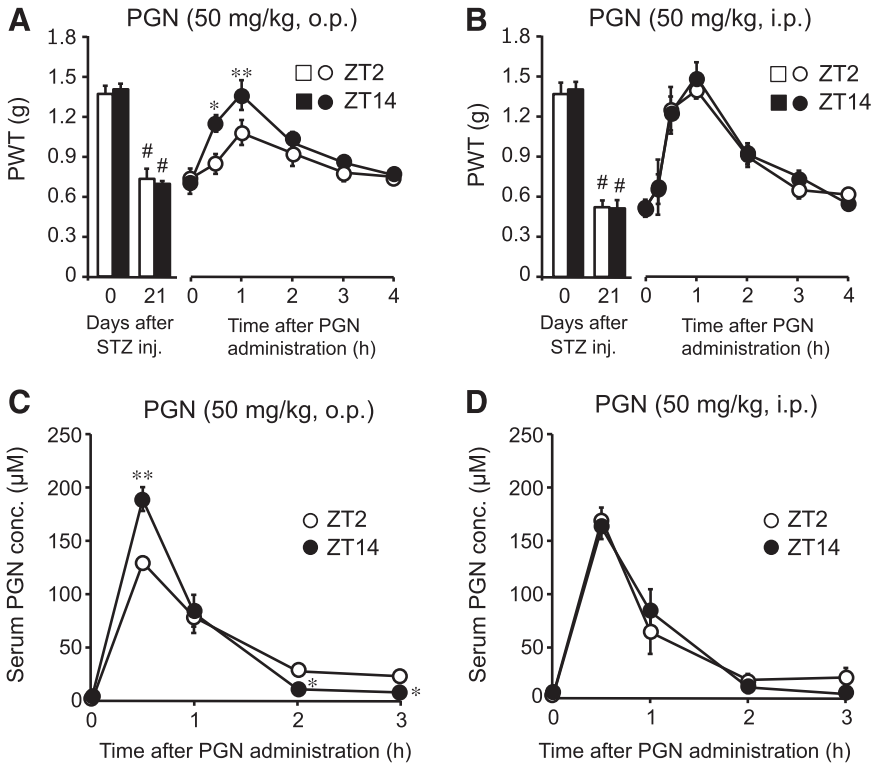

Fig. 2. Influence of the dosing time on analgesic effects of PGN in STZ-induced diabetic mice (A and B). The time course of PWT in STZ-induced diabetic mice after the oral (A) or intraperitoneal (B) administration of PGN (50 mg/kg) at ZT2 and ZT14 (C and D). The time course of serum concentrations of PGN in STZ-induced diabetic mice after the oral (C) or intraperitoneal (D) administration of PGN (50 mg/kg) at ZT2 and ZT14. These experiments were performed on day 21 after the STZ treatment. Values are shown as means with S.E.M. (n = 4–13). $^{\#}P < 0.01$, significantly different from the value of day 0 at the corresponding time points. $^{**}P < 0.01$, $^{*}P < 0.05$, significantly different from the value for the ZT2 administration.

accumulation of the drug (Fig. 3A, right). The accumulation of PGN was further enhanced in Octn1-overexpressing aMoS7 cells. Consistent with previous observation (Tamai et al., 2000), the uptake of PGN into Octn1-overexpressing aMoS7 cells showed in a sodium-dependent manner (Fig. 3B). Similar sodium dependence was also observed in the uptake of PGN in native aMoS7 cells. Concomitant incubation with a typical Octn1 substrate ERGO prevented significantly the uptake of PGN not only into Octn1-overexpressing cells but also into native aMoS7 cells (Fig. 3C). These results suggest that Octn1 can transport PGN into the cells. The uptake of PGN into the cells was due, at least partly, to Octn1. This notion was also supported by the fact that downregulation of Octn1 by siRNA decreased PGN incorporation into the native aMoS7 cells (Fig. 3D).

On day 21 after the STZ treatment, the protein levels of Octn1 showed obvious circadian oscillations in the small intestine of STZ-induced diabetic mice with peak levels occurring around the early dark phase (Fig. 4A). The rhythmicity in the intestinal expression of Octn1 in STZ-induced diabetic mice was similar to that observed in control healthy mice. After the incubation of jejunal segments prepared from STZ-induced diabetic mice with 0.5 mM PGN, the accumulation of the compound in the intestinal epithelial cells showed significant time-dependent variations (Fig. 4B). The amount of PGN incorporation was significantly higher at ZT14 than at ZT2 ($P < 0.01$). Because variations in the intestinal accumulation of PGN were dampened when the segments were incubated in the presence of 0.5 mM ERGO, dosing time-dependent differences in the intestinal absorption of PGN appeared to be caused by the circadian expression of Octn1.

The Temporal Expression of $\alpha 2\delta$-1 Subunits in the Spinal Cord of STZ-Induced Diabetic Mice. The dosing time dependency of the pharmacologic effects of drugs is attributable not only to circadian changes in their pharmacokinetics but also to the rhythmic expression of their target molecule (Kusunose et al., 2010). PGN is an effective analgesic because it modulates Ca^{2+} currents by binding to the $\alpha 2\delta$-1 subunits of voltage-dependent Ca^{2+} channels in the

TABLE 1

Influence of dosing times on pharmacokinetic parameters after the oral administration of PGN (50 mg/kg) at ZT2 or ZT14

Values are the mean ± S.E.M. of 58 mice. Significant differences between the two groups were evaluated by the Student's t-test. The 1% level of probability was considered to be significant.

Pharmacokinetic Parameters	Time of Drug Administration		Significance
	ZT2	ZT14	
CL/F (l/h/kg)	1.399 ± 0.039	1.337 ± 0.035	N.S.
AUC (μg•h/ml)	36.556 ± 1.031	38.289 ± 1.183	N.S.
k_e (h)	10.315 ± 0.295	9.847 ± 0.275	N.S.
k_a (h)	0.858 ± 0.029	1.795 ± 0.066	$P < 0.01$
$t_{1/2}$ (h)	0.069 ± 0.002	0.072 ± 0.002	N.S.

CL, clearance; k_a, absorption rate constant; k_e, elimination rate constant; N.S., not significant.

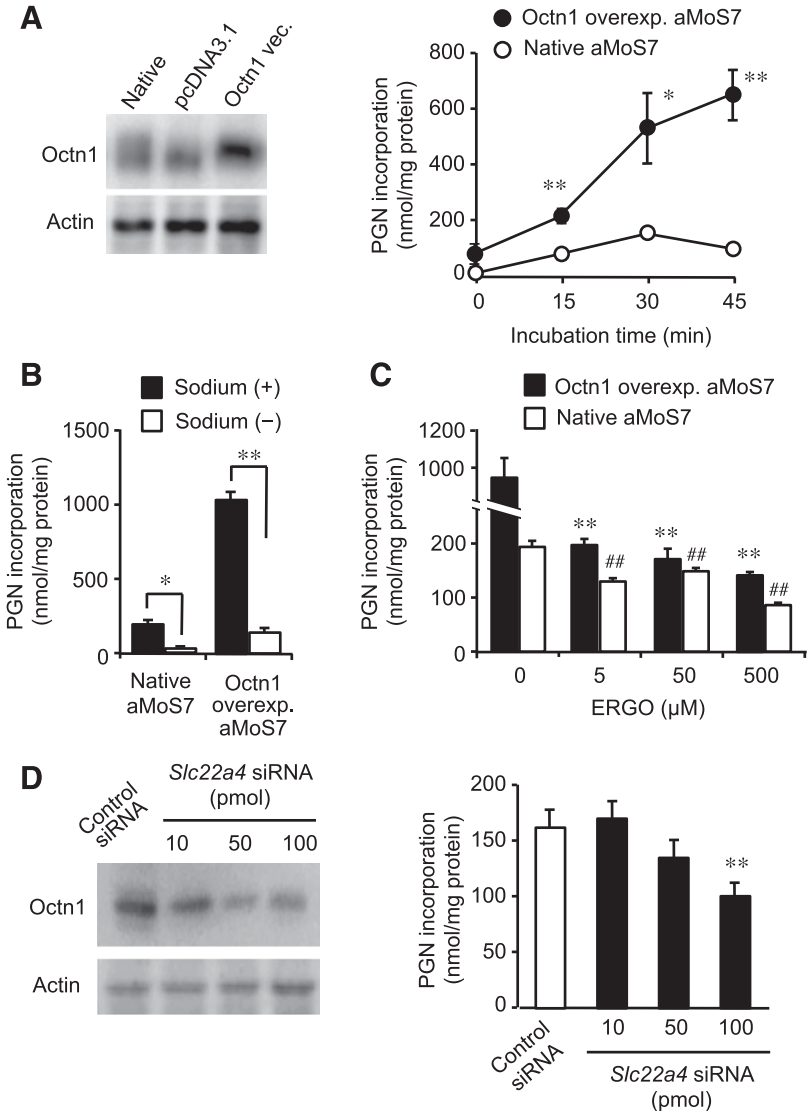

Fig. 3. Octn1 mediates the uptake of PGN into the intestinal epithelial cells. (A) Enhancement of PGN incorporation into aMoS7 cells by overexpression of Octn1. Left panel photograph shows Western blot analysis of stable expression of Octn1 in aMoS7 cells. Cells were transfected with empty (pcDNA3.1) or Octn1-expressing vectors (Octn1 vec.). Right panel shows time course of PGN uptake into native or Octn1-overexpressing cells. Cells were incubated with 30 mM PGN for indicated times. Values are shown as means with S.E.M. (n = 3). $^{**}P < 0.01$, $^{*}P < 0.05$, significantly different from native aMoS7 cells at the corresponding time points. (B) Sodium dependence of PGN uptake by native and Octn1-overexpressing aMoS7 cells. Cells were incubated with 30 mM PGN for 30 minutes in the presence or absence of sodium. Values are shown as means with S.E.M. (n = 3 or 4). $^{**}P < 0.01$, $^{*}P < 0.05$ significantly different between the two groups. (C) Inhibition of PGN uptake into aMoS7 cells by ERGO. Native and Octn1-overexpressing aMoS7 cells were concomitantly incubated with 30 mM PGN and ERGO at indicated concentrations for 30 minutes. Values are shown as means with S.E.M. (n = 4). $^{**}P < 0.01$, $^{\#\#}P < 0.01$ significantly different from untreated groups (0 μM). (D) Downregulation of Octn1 diminishes the uptake of PGN into aMoS7 cells. Native aMoS7 cells were transfected with scrambled siRNA (Control siRNA) or specific siRNA against the *Slc22a4* gene. The incorporation of PGN and expression of Octn1 were assessed 48 hours after transfection. Values are shown as means with S.E.M. (n = 4 or 5). $^{**}P < 0.01$, significantly different from control siRNA-transfected groups.

spinal cord (Fink et al., 2002). However, on day 21 after the STZ treatment, the protein levels of $\alpha 2\delta$-1 subunits in the spinal cord of STZ-induced diabetic mice did not show significant time-dependent oscillations. The temporal expression profile of the $\alpha 2\delta$-1 protein in STZ-induced diabetic mice was similar to that in normal healthy mice (Fig. 4C).

Dosing Time Dependency of Analgesic Effects of PGN in Diabetic db/db Mice. In the final set of experiments, we investigated whether the analgesic effects of PGN were also changed in type II diabetic mice by dosing in a time-dependent manner. To achieve this, db/db mice were used as a model of type II diabetes. Blood glucose levels and body weights of db/db mice increased gradually (Fig. 5, A and B) and exhibited the pathologic phenotype of type II diabetes. The PWT of diabetic db/db mice started to decrease when animals were 6 weeks old. The significant and stable decrease in the pain threshold was observed in 10-week-old mice (Fig. 5C). When diabetic db/db mice were 12 weeks old, the analgesic effects of PGN were tested by oral administration (50 mg/kg). Although the PWT of diabetic db/db mice was significantly increased after administration of PGN at both dosing time points, there was no significant different in the PWT between the two times (Fig. 6A). Before administration of PGN, the PWT of diabetic db/db mice showed time-dependent variation. This could hinder an accurate comparison of analgesic effects of PGN between two dosing times. Therefore, we also evaluated the analgesic effects of PGN by setting the baseline of PWT at 1.0. The normalized PWT of mice 0.5, 1, 2, and 3 hours after the administration of PGN at ZT14 was significantly higher than that at ZT2 (Fig. 6B, left). The normalized AUC of the PWT after PGN administration at ZT14 was also significantly larger than that after the drug administration at ZT2 ($P < 0.01$; Fig. 6B, right), suggesting that the analgesic effects of PGN in diabetic db/db mice were potent when mice were administrated the drug at the early dark phase. This result was consisted with the dosing time dependency of the analgesic effects of PGN observed in STZ-induced diabetic mice (Fig. 2A).

The intestinal expression of the Octn1 protein in diabetic db/db mice also showed circadian oscillations, with peak levels around the early dark phase (Fig. 6C). This expression pattern was similar to that observed in wild-type mice and STZ-induced diabetic mice. These results suggested that the dosing time-dependent difference observed in the analgesic

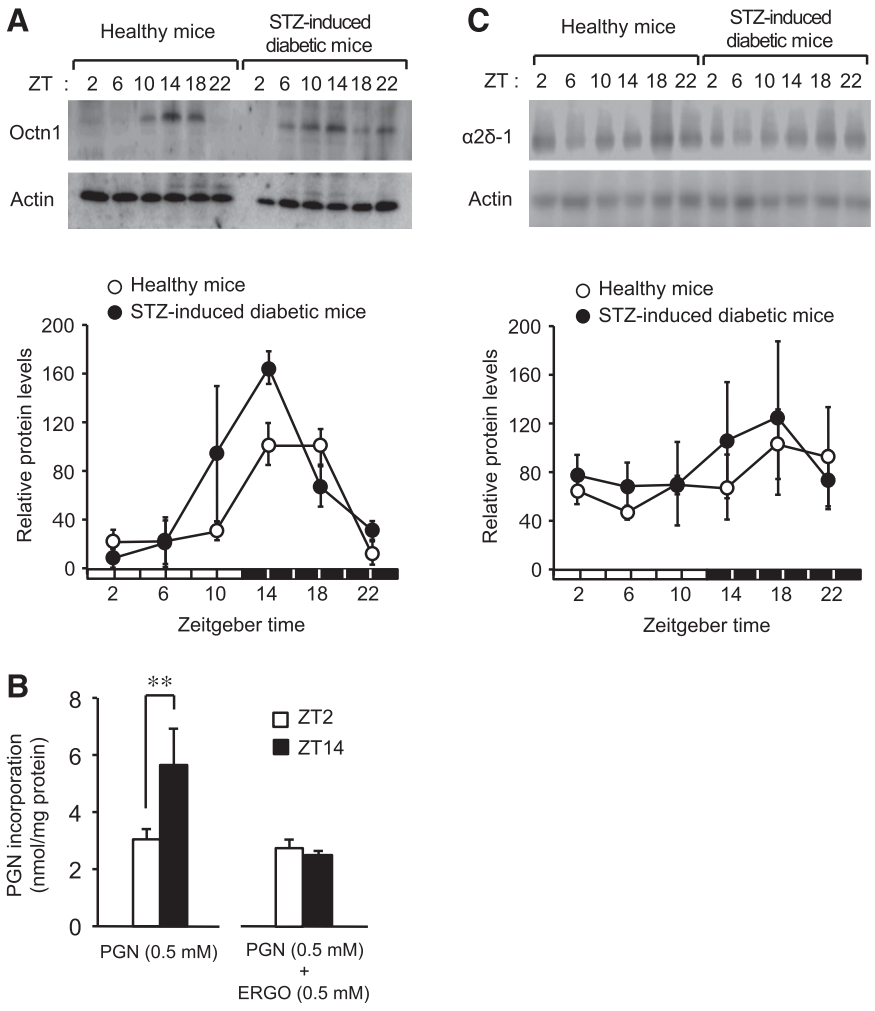

Fig. 4. Temporal profiles of intestinal expression of Octn1 and spinal expression of $\alpha 2\delta$-1 protein in STZ-induced diabetic mice. (A) Circadian expression of the Octn1 protein in the small intestine of healthy and STZ-induced diabetic mice. (Upper) Representative photograph of Western blotting of Octn1. Values are shown as means with S.E.M. (n = 6). There are significant time-dependent differences in the protein levels of Octn1 in healthy and STZ-induced diabetic mice ($P < 0.01$ for healthy mice and $P < 0.05$ for diabetic mice; analysis of variance). (B) The time-dependency of PGN accumulation in the small intestine of STZ-induced diabetic mice. Jejunal segments were incubated with 0.5 mM PGN in the presence or absence of 0.5 mM ERGO. Values are shown as means with S.E.M. (n = 6). $^{**}P < 0.01$, significant difference between two groups. (C) Temporal expression profiles of the $\alpha 2\delta$-1 protein in the spinal cord of healthy and STZ-induced diabetic mice. (Upper) Representative photograph of Western blotting of $\alpha 2\delta$-1. The experiments were performed on day 21 after the STZ treatment. Values are shown as means with S.E.M. (n = 6). Protein levels of Octn1 and $\alpha 2\delta$-1 were normalized to Actin, and peak levels of healthy groups were set at 100.

effects of PGN in diabetic db/db mice were also caused by circadian changes in the pharmacokinetic process.

Discussion

Because of daily variations in biologic functions, many drugs cannot be expected to have the same efficacy at different administration times. Accumulating the evidence reveals that circadian changes in the sensitivity of living organisms to drugs and their pharmacokinetics affect the effectiveness of drugs (Matsunaga et al., 2008; Murakami et al., 2008).

In the present study, we demonstrated that the analgesic effects of PGN after its oral administration were changed in STZ-induced diabetic mice. The analgesic effects of PGN were more potent in mice treated with the drug at ZT14 than at ZT2. Furthermore, the peak concentrations of PGN in STZ-induced diabetic mice were significantly higher after its oral administration at ZT14 than at ZT2. On the other hand, dosing time-dependent differences in the analgesic effects of PGN and its serum concentrations were not observed after its intraperitoneal administration to diabetic db/db mice. These results suggested that circadian changes in the pharmacokinetics of

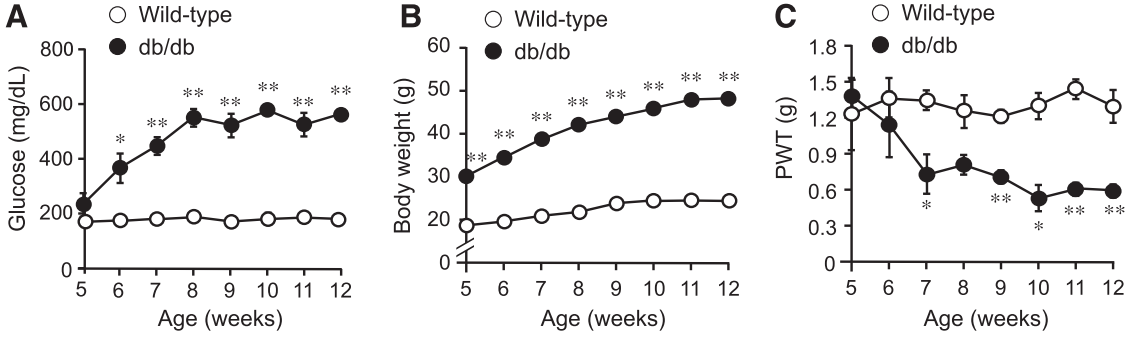

Fig. 5. Development of diabetic neuropathy in db/db mice. The time courses of blood glucose levels (A), body weight (B), and PWT (C) in db/db mice. Values are shown as means with S.E.M. (n = 6 or 7). $^{**}P < 0.01$, $^{*}P < 0.05$, significantly different from wild-type mice at the corresponding time points.

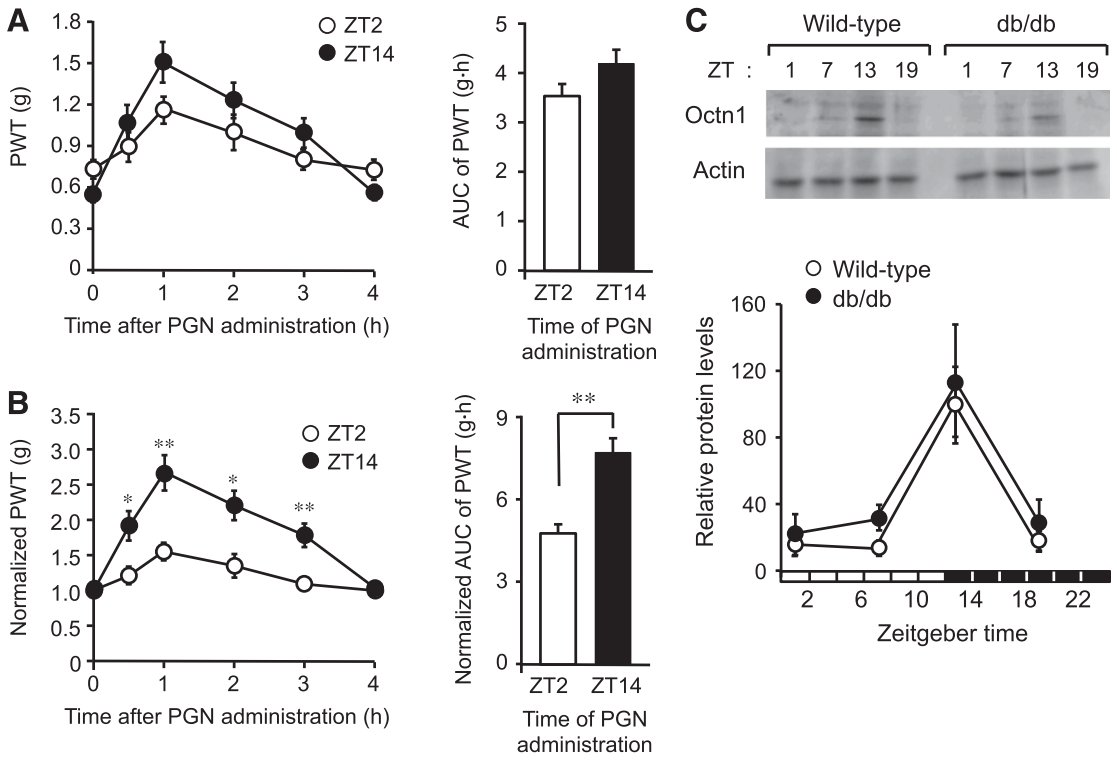

Fig. 6. Dosing time dependency of analgesic effects of PGN in diabetic db/db mice. (A) (Left) Time course of PWT in db/db mice after the oral administration of PGN (50 mg/kg) at ZT2 and ZT14. (Right) Comparison of the AUC of PWT. The AUC of PWT after PGN administration was calculated using trapezoidal rule. (B) (Left) Time course of normalized PWT (basal values are set at 1.0) in db/db mice after the oral administration of PGN (50 mg/kg) at ZT2 and ZT14. (Right) Comparison of the normalized AUC of PWT. Values are shown as means with S.E.M. ($n = 6$). $^{**}P < 0.01$, $^{*}P < 0.05$ compared with ZT2-treated groups. (C) Temporal expression profiles of the Octn1 protein in the small intestine of wild-type and db/db mice. Intestinal proteins were extracted from 12-week-old mice. Values are shown as means with S.E.M. ($n = 6$). Protein levels of Octn1 were normalized to Actin and peak levels of wild-type mice were set at 100. There are significant time-dependent differences in the protein levels of Octn1 in wild-type and db/db mice ($P < 0.01$ for wild-type mice and $P < 0.05$ for db/db mice; analysis of variance).

PGN after its oral administration caused the dosing time-dependent difference observed in its analgesic effects in STZ-induced diabetic mice.

Pharmacokinetic processes have been broadly separated into absorption, distribution, metabolism, and elimination. To determine the contribution of these pharmacokinetic processes to circadian changes in the pharmacokinetics of PGN, we analyzed serum concentrations of orally administrated PGN in STZ-induced diabetic mice by the NONMEM program. In this analysis, pharmacokinetic parameters were determined after the one-compartment model with first-order absorption. The dosing time-dependent difference in the serum concentrations of PGN was attributed to circadian changes in the absorption rate constant (k_a). This result of the pharmacokinetic analysis was consistent with the dosing time-dependent difference observed in the peak serum concentration of PGN in mice after its oral, but not intraperitoneal, administration in the present study.

The small intestine is a major organ for the absorption of drugs after their oral administration, and various types of transporters are expressed on intestinal epithelial cells that positively and/or negatively contribute to intestinal drug absorption (Tsuji and Tamai, 1996; Bleasby et al., 2006; Stearns et al., 2008). The intestinal absorption of PGN has also been suggested to be mediated by several types of transporters (Jezyk et al., 1999; Piyapolrungroj et al., 2001). Three types of Octn transporters have been identified in mice (Tamai et al., 2000). The expression of Octn1 and Octn2 is detected in several tissues in human and mice, but Octn3 is specifically expressed in mouse testis (Lamhonwah et al., 2003). Although both Octn1 and Octn2 exhibit sodium-dependent carnitine transport, Octn3 is a sodium-independent carnitine transporter (Tamai et al., 2000). Among them, Octn1 is the most attractive candidate as a mediator for the intestinal absorption of PGN, because the incorporation of gabapentin, a structural analog of PGN, into intestinal epithelial cells is mediated by Octn1 (Wada et al., 2015). The result of the up- or downregulation experiment using cultured mouse intestinal epithelial cells suggested that the uptake of PGN into aMoS7 cells was also mediated by Octn1. Furthermore, the contribution of Octn1 to the intestinal absorption of PGN was supported by the fact that a typical Octn1's substrate ERGO inhibited the uptake of PGN into cultured mouse intestinal epithelial cells and the jejunal segments of STZ-induced diabetic mice. In laboratory animals, the expression and functions of several types of intestinal transporters have been shown to exhibit circadian oscillations (Murakami et al., 2008; Hamdan et al., 2012; Okamura et al., 2014). The expression of Octn1 in the intestines of mice was found to oscillate in a circadian time-dependent manner (Wada et al., 2015). Concomitant incubation of the jejunal segments with 0.5 mM ERGO abrogated the time-dependent variation in the uptake of PGN, the treatment failed to suppress completely the uptake of PGN into the jejunal segments. Although the data suggest that other types of transporters, whose intestinal expression is constant the day, also mediate the uptake of PGN into intestinal epithelial cells, time dependency of PGN uptake into small intestine of mice is

mainly due to circadian expression of Octn1. The enhanced expression of Octn1 during the early dark phase appears to facilitate the uptake of PGN into intestinal epithelial cells. The time-dependent suppression of peroxisome proliferator-activated receptor-α activity by bile acids underlies the circadian expression of Octn1 (Wada et al., 2015). Although both STZ-induced diabetic mice and db/db mice increase food intake, they still consumed more amount of food during the dark phase (Laposky et al., 2008; Bostwick et al., 2010). Therefore, the day/night difference in intestinal accumulated bile acids caused circadian changes in peroxisome proliferator-activated receptor-α activity, resulting in the time-dependent expression of Octn1 in the small intestine of diabetic mice.

From the perspective of pharmacodynamics, the temporal expression profile of $\alpha2\delta$-1 subunits was also assessed in the spinal cord of STZ-induced diabetic mice. A previous study suggests that the circadian expression of $\alpha2\delta$-1 subunits in the spinal cord of nerve-injured mice contributes to dosing time-dependent changes in the analgesic effects of gabapentin (Kusunose et al., 2010). However, protein levels of $\alpha2\delta$-1 subunits in the spinal cord of STZ-induced diabetic mice did not show significant time-dependent oscillations. Therefore, it is unlikely that the dosing time-dependent difference observed in the analgesic effects of PGN was associated with the function of voltage-dependent Ca^{2+} channels.

Diabetes has been separated into type I and type II according to the cause of disease. Leptin receptor-deficient db/db mice are often used as a model of type II diabetes. The analgesic effects of PGN in db/db mice were significantly greater after its oral administration at ZT14 than at ZT2. Furthermore, the intestinal expression of the Octn1 protein in db/db mice also showed circadian oscillations, with peak levels being observed around the early dark phase. Therefore, circadian changes in the intestinal absorption process may also underlie the dosing time-dependent difference in the analgesic effects of PGN in diabetic db/db mice.

The results of the present study provide a clearer understanding of how the analgesic effects of PGN on diabetes-induced peripheral neuropathic pain vary according to its dosing time. The dosing time-dependent change in the analgesic effects of PGN was observed in both type I and type II diabetic model mice. Advancements in understanding circadian changes in the intestinal absorption process appear to be important for predicting the dosing time-dependency of the analgesic effects of PGN. Furthermore, the results of the present study suggest that the therapeutic efficacy of PGN on diabetic peripheral neuropathic pain may be improved by optimizing the dosing schedule.

Authorship Contributions

Participated in research design: Akamine, Koyanagi, Ohdo.
Conducted experiments: Akamine, Koyanagi, Kusunose, Taniguchi.
Contributed new reagents or analytic tools: Akamine, Matsunaga.
Performed data analysis: Akamine, Koyanagi, Hashimoto.
Wrote or contributed to the writing of the manuscript: Akamine, Koyanagi, Ohdo.

References

Blay RA, Bigley NJ, and Giron DJ (1985) A murine model of insulin-dependent diabetes mellitus resulting from the cumulative effects of the nondiabetogenic strain of encephalomyocarditis virus and a single low dose of streptozocin. *Diabetes* **34**:1288–1292.

Bleasby K, Castle JC, Roberts CJ, Cheng C, Bailey WJ, Sina JF, Kulkarni AV, Hafey MJ, Evers R, Johnson JM, et al. (2006) Expression profiles of 50 xenobiotic transporter genes in humans and pre-clinical species: a resource for investigations into drug disposition. *Xenobiotica* **36**:963–988.

Bostwick J, Nguyen D, Cornélissen G, Halberg F, and Hoogerwerf WA (2010) Effects of acute and chronic STZ-induced diabetes on clock gene expression and feeding in the gastrointestinal tract. *Mol Cell Biochem* **338**:203–213.

Chaplan SR, Bach FW, Pogrel JW, Chung JM, and Yaksh TL (1994) Quantitative assessment of tactile allodynia in the rat paw. *J Neurosci Methods* **53**:55–63.

Dooley DJ, Donovan CM, Meder WP, and Whetzel SZ (2002) Preferential action of gabapentin and pregabalin at P/Q-type voltage-sensitive calcium channels: inhibition of K^+-evoked [^{3}H]-norepinephrine release from rat neocortical slices. *Synapse* **45**:171–190.

Fink K, Dooley DJ, Meder WP, Suman-Chauhan N, Duffy S, Clusmann H, and Göthert M (2002) Inhibition of neuronal $Ca^{(2+)}$ influx by gabapentin and pregabalin in the human neocortex. *Neuropharmacology* **42**:229–236.

Gachon F, Nagoshi E, Brown SA, Ripperger J, and Schibler U (2004) The mammalian circadian timing system: from gene expression to physiology. *Chromosoma* **113**: 103–112.

Gründemann D, Harlfinger S, Golz S, Geerts A, Lazar A, Berkels R, Jung N, Rubbert A, and Schömig E (2005) Discovery of the ergothioneine transporter. *Proc Natl Acad Sci USA* **102**:5256–5261.

Hamdan AM, Koyanagi S, Wada E, Kusunose N, Murakami Y, Matsunaga N, and Ohdo S (2012) Intestinal expression of mouse Abcg2/breast cancer resistance protein (BCRP) gene is under control of circadian clock-activating transcription factor-4 pathway. *J Biol Chem* **287**:17224–17231.

Iwamoto T, Yamada K, Shimizu M, and Totsuka M (2011) Establishment of intestinal epithelial cell lines from adult mouse small and large intestinal crypts. *Biosci Biotechnol Biochem* **75**:925–929.

Jezyk N, Li C, Stewart BH, Wu X, Bockbrader HN, and Fleisher D (1999) Transport of pregabalin in rat intestine and Caco-2 monolayers. *Pharm Res* **16**:519–526.

Kavoussi R (2006) Pregabalin: From molecule to medicine. *Eur Neuropsychopharmacol* **16** (Suppl 2):S128–S133.

Kusunose N, Koyanagi S, Hamamura K, Matsunaga N, Yoshida M, Uchida T, Tsuda M, Inoue K, and Ohdo S (2010) Molecular basis for the dosing time-dependency of anti-allodynic effects of gabapentin in a mouse model of neuropathic pain. *Mol Pain* **6**:83–90.

Lamhonwah AM, Skaug J, Scherer SW, and Tein I (2003) A third human carnitine/organic cation transporter (OCTN3) as a candidate for the 5q31 Crohn's disease locus (IBD5). *Biochem Biophys Res Commun* **301**:98–101.

Laposky AD, Bradley MA, Williams DL, Bass J, and Turek FW (2008) Sleep-wake regulation is altered in leptin-resistant (db/db) genetically obese and diabetic mice. *Am J Physiol Regul Integr Comp Physiol* **295**:R2059–R2066.

Lemmer B (2005) Chronopharmacology and controlled drug release. *Expert Opin Drug Deliv* **2**:667–681.

Lévi F, Zidani R, and Misset JL (1997) Randomised multicentre trial of chronotherapy with oxaliplatin, fluorouracil, and folinic acid in metastatic colorectal cancer. *Lancet* **350**:681–686.

Matsunaga N, Ikeda M, Takiguchi T, Koyanagi S, and Ohdo S (2008) The molecular mechanism regulating 24-hour rhythm of CYP2E1 expression in the mouse liver. *Hepatology* **48**:240–251.

Murakami Y, Higashi Y, Matsunaga N, Koyanagi S, and Ohdo S (2008) Circadian clock-controlled intestinal expression of the multidrug-resistance gene mdr1a in mice. *Gastroenterology* **135**:1636–1644.

Ohdo S, Koyanagi S, Suyama H, Higuchi S, and Aramaki H (2001) Changing the dosing schedule minimizes the disruptive effects of interferon on clock function. *Nat Med* **7**:356–360.

Okamura A, Koyanagi S, Dilxiat A, Kusunose N, Chen JJ, Matsunaga N, Shibata S, and Ohdo S (2014) Bile acid-regulated peroxisome proliferator-activated receptor-α (PPARα) activity underlies circadian expression of intestinal peptide absorption transporter PepT1/Slc15a1. *J Biol Chem* **289**:25296–25305.

Parker L, Huelin R, Khankhel Z, Wasiak R, and Mould J (2015) A systematic review of pharmacoeconomic studies for pregabalin. *Pain Pract* **15**:82–94.

Piyapolrungroj N, Li C, Bockbrader H, Liu G, and Fleisher D (2001) Mucosal uptake of gabapentin (neurontin) vs. pregabalin in the small intestine. *Pharm Res* **18**: 1126–1130.

Rosenstock J, Tuchman M, LaMoreaux L, and Sharma U (2004) Pregabalin for the treatment of painful diabetic peripheral neuropathy: a double-blind, placebo-controlled trial. *Pain* **110**:628–638.

Stearns AT, Balakrishnan A, Rhoads DB, Ashley SW, and Tavakkolizadeh A (2008) Diurnal rhythmicity in the transcription of jejunal drug transporters. *J Pharmacol Sci* **108**:144–148.

To H, Yoshimatsu H, Tomonari M, Ida H, Tsurumoto T, Tsuji Y, Sonemoto E, Shimasaki N, Koyanagi S, Sasaki H, et al. (2011) Methotrexate chronotherapy is effective against rheumatoid arthritis. *Chronobiol Int* **28**:267–274.

Tamai I, Ohashi R, Nezu JI, Sai Y, Kobayashi D, Oku A, Shimane M, and Tsuji A (2000) Molecular and functional characterization of organic cation/carnitine transporter family in mice. *J Biol Chem* **275**:40064–40072.

Tsuji A and Tamai I (1996) Carrier-mediated intestinal transport of drugs. *Pharm Res* **13**:963–977.

Vermeij TA and Edelbroek PM (2004) Simultaneous high-performance liquid chromatographic analysis of pregabalin, gabapentin and vigabatrin in human serum by precolumn derivatization with *o*-phtaldialdehyde and fluorescence detection. *J Chromatogr B Analyt Technol Biomed Life Sci* **810**:297–303.

Wada E, Koyanagi S, Kusunose N, Akamine T, Masui H, Hashimoto H, Matsunaga N, and Ohdo S (2015) Modulation of peroxisome proliferator-activated receptor-α activity by bile acids causes circadian changes in the intestinal expression of Octn1/*Slc22a4* in mice. *Mol Pharmacol* **87**:314–322.

Address correspondence to: Dr. Shigehiro Ohdo, Department of Pharmaceutics, Faculty of Pharmaceutical Sciences, Kyushu University, 3-1-1 Maidashi Higashi-ku, Fukuoka 812-8582, Japan. E-mail: ohdo@phar.kyushu-u.ac.jp